

Correlation Functions of Net-proton Multiplicity Distributions in Au + Au Collisions at RHIC Energies from AMPT Model

Yufu Lin,¹ Lizhu Chen,² and Zhiming Li^{1,*}

¹*Key Laboratory of Quark and Lepton Physics (MOE) and Institute of Particle Physics,
Central China Normal University, Wuhan 430079, China*

²*School of Physics and Optoelectronic Engineering,
Nanjing University of Information Science and Technology, Nanjing 210044, China*

Fluctuations of conserved quantities are believed to be sensitive observables to probe the signature of QCD phase transition and critical point. It is argued recently that measuring the genuine correlation functions (CF) could provide cleaner information on possible non-trivial dynamics in heavy-ion collisions. With the AMPT model, the centrality and energy dependence of various orders of CFs of net-proton in Au+Au collisions at $\sqrt{s_{NN}}=7.7, 11.5, 19.6, 27, 39, 62.4$ and 200 GeV are investigated. The model results show that the number of anti-proton is important and should be taken into account in the calculation of CFs in high energy and/or at peripheral collisions. It is also found that the contribution of anti-proton is more important for higher order correlations than for lower ones. The CFs of anti-protons and mix-correlations play comparable roles to those of protons in high energies. Finally, we make comparisons between the model calculation and experimental data measured by STAR at the BNL Relativistic Heavy Ion Collider.

I. INTRODUCTION

The search for the structure of the QCD phase diagram is one of the main goals in relativistic heavy-ion collisions [1, 2]. Event-by-event fluctuations of conserved quantities are less affected by final state interaction in the hadronic phase and thus have been believed to be sensitive to the QCD critical point [3–9]. With the data collected from the first beam energy scan (BES-I) program at Relativistic Heavy Ion Collider (RHIC), cumulants of net-proton, net-charge, and net-kaon multiplicity distributions have been measured [10–16]. A non-monotonic energy dependence of the cumulant ratio of the fourth order to the second order ($\kappa\sigma^2$) for net-proton in central Au+Au collisions has been observed in STAR experiment, with a minimum value around 19.6 GeV, and a strong enhancement at 7.7 and 11.5 GeV [17, 18].

Recently, it is argued [19–23] that measuring multiparticle correlation function could provide cleaner information on the dynamics of critical fluctuations in heavy-ion collisions since cumulant may mix correlations of different orders. By ignoring the contributions from anti-protons, various orders of correlation functions between protons can be extracted from the cumulants measured by the STAR experiment. It is found that the strong enhancement of forth order cumulant at 7.7 GeV is due to large four-particle correlations, while the negative two-particle correlations are dominant at 19.6 GeV [21]. With removal of the four-particle correlation function from the cumulants, i.e., only the two- and three-particle correlation functions remain, the non-monotonic behavior observed in the forth order proton cumulant disappears [24]. The UrQMD Model can not explain the observed behav-

iors of the proton correlation functions from STAR [25]. The correlation functions could also be effectively used to study the long-range correlations of the system [26] and describe the asymmetric component of rapidity correlations measured by the ATLAS experiment [27, 28].

It should be pointed out that proton number is not a conserved charge although the number of anti-proton is comparable small and may be neglected at very low RHIC energies. With increasing collision energies, the experimentally measured anti-proton to proton ratio (\bar{p}/p) increases dramatically [29], and we should consider the contribution from anti-proton as well as that from proton when calculating cumulants or correlation functions. On the other hand, the mixed correlation functions between proton and anti-proton may carry important information about the system under investigation. In ref [30] it is suggested that measurement of these mixed correlations could help to identify the possible origination of proton clustering, which can be used to qualitatively understand the preliminary STAR results for multi-particle correlation functions of different orders.

In this work, we plan to perform a study on the correlation functions of net-proton by taking both proton and anti-proton into account. The correlation functions of net-proton at various RHIC BES energies and centralities are investigated and compared to those of proton only. We also make comparisons of correlation functions from proton or anti-proton to those from mixed correlations. The contributions of anti-proton numbers to various orders of correlation functions are systematically studied. The paper is organized as follows. In Sec.II, we introduce the observables and relations between cumulant, factorial moment and correlation function. A brief introduction of AMPT model is given in Sec.III. Then, the centrality dependence of various orders of correlation functions of net-proton, only proton or anti-proton and mix-correlation are investigated by AMPT model in Au+Au collisions at $\sqrt{s_{NN}}=7.7$ to 200 GeV. Finally, we give a summary to

*Electronic address: lizm@mail.ccnu.edu.cn

this work.

II. CUMULANT, FACTORIAL MOMENT AND CORRELATION FUNCTION

In statistics, the distribution function of a measurement can be characterized by various orders of cumulants. The n th order cumulants (C_n) of an multiplicity distribution can be defined as:

$$\begin{aligned} C_1 &= \langle N \rangle \\ C_2 &= \langle (\delta N)^2 \rangle \\ C_3 &= \langle (\delta N)^3 \rangle \\ C_4 &= \langle (\delta N)^4 \rangle - 3\langle (\delta N)^2 \rangle^2 \end{aligned} \quad (1)$$

where N represents the number of multiplicities measured in one event and $\delta N = N - \langle N \rangle$ denotes the deviation of N to its mean value. The measurement N could be the number of proton, anti-proton or net-proton.

In order to cancel the volume effect, the ratio of the fourth order to the second order cumulants, $\kappa\sigma^2$, is often used to study the non-monotonic behavior in current heavy-ion experiments [10–12]. It can be obtained by:

$$\kappa\sigma^2 = \frac{C_4}{C_2} \quad (2)$$

Suppose that the final state particles are characterized by the multiplicity distribution $P(N)$, where N is only one species of particles, such as protons. The n -th order factorial moment $F_n = \langle N!/(N-n)! \rangle$ can be calculated from the generating function $H(z)$:

$$F_n = \frac{d^n}{dz^n} H(z)|_{z=1}, H(z) = \sum_N P(N) z^N. \quad (3)$$

The n -th order correlation function, $\hat{\kappa}_n$, is then given by analogous derivatives of the logarithm of $H(z)$,

$$\hat{\kappa}_n = \frac{d^n}{dz^n} \ln[H(z)]|_{z=1}. \quad (4)$$

The correlations functions can be obtained from the factorial moments:

$$\begin{aligned} \hat{\kappa}_1 &= F_1 \\ \hat{\kappa}_2 &= F_2 - F_1^2 \\ \hat{\kappa}_3 &= F_3 - 3F_1F_2 + 2F_1^3 \\ \hat{\kappa}_4 &= F_4 - 4F_1F_3 - 3F_2^2 + 12F_1^2F_2 - 6F_1^4 \end{aligned} \quad (5)$$

In the mean time, cumulants can also be expressed in terms of the factorial moments [20, 23]. Thus, cumulants

and correlation functions have directly connections with each other:

$$C_2 = \langle N \rangle + \hat{\kappa}_2 \quad (6)$$

$$C_3 = \langle N \rangle + 3\hat{\kappa}_2 + \hat{\kappa}_3 \quad (7)$$

$$C_4 = \langle N \rangle + 7\hat{\kappa}_2 + 6\hat{\kappa}_3 + \hat{\kappa}_4 \quad (8)$$

It can be clearly seen that cumulants mix correlations of different orders. For example, from Eq. (8) we find that the forth-order cumulant mix up the second-, third- and fourth-order correlation functions.

We must point out that the above relationships are valid only when one type of particle, such as proton, is taken into account. For net-proton, i.e. both proton and anti-proton are considered, the relationship between correlation functions and factorial moments can be deduced [20]:

$$\begin{aligned} \hat{\kappa}_2^{(2,0)} &= F_{2,0} - F_{1,0}^2 \\ \hat{\kappa}_2^{(0,2)} &= F_{0,2} - F_{0,1}^2 \\ \hat{\kappa}_2^{(1,1)} &= F_{1,1} - F_{1,0}F_{0,1} \\ \hat{\kappa}_3^{(3,0)} &= F_{3,0} - 3F_{1,0}F_{2,0} + 2F_{1,0}^3 \\ \hat{\kappa}_3^{(0,3)} &= F_{0,3} - 3F_{0,1}F_{0,2} + 2F_{0,1}^3 \\ \hat{\kappa}_3^{(2,1)} &= F_{2,1} - F_{0,1}F_{2,0} - 2F_{1,0}F_{1,1} + 2F_{0,1}F_{1,0}^2 \\ \hat{\kappa}_3^{(1,2)} &= F_{1,2} - F_{1,0}F_{0,2} - 2F_{0,1}F_{1,1} + 2F_{1,0}F_{0,1}^2 \\ \hat{\kappa}_4^{(4,0)} &= F_{4,0} - 4F_{1,0}F_{3,0} - 3F_{2,0}^2 + 12F_{1,0}^2F_{2,0} - 6F_{1,0}^4 \\ \hat{\kappa}_4^{(0,4)} &= F_{0,4} - 4F_{0,1}F_{0,3} - 3F_{0,2}^2 + 12F_{0,1}^2F_{0,2} - 6F_{0,1}^4 \\ \hat{\kappa}_4^{(3,1)} &= F_{3,1} - F_{0,1}F_{3,0} - 3F_{1,0}F_{2,1} - 3F_{1,1}F_{2,0} \\ &\quad + 6F_{0,1}F_{1,0}F_{2,0} + 6F_{1,0}^2F_{1,1} - 6F_{0,1}F_{1,0}^3 \\ \hat{\kappa}_4^{(1,3)} &= F_{1,3} - F_{1,0}F_{0,3} - 3F_{0,1}F_{1,2} - 3F_{1,1}F_{0,2} \\ &\quad + 6F_{1,0}F_{0,1}F_{0,2} + 6F_{0,1}^2F_{1,1} - 6F_{1,0}F_{0,1}^3 \\ \hat{\kappa}_4^{(2,2)} &= F_{2,2} - 2F_{0,1}F_{2,1} + (2F_{0,1}^2 - F_{0,2})F_{2,0} - 2F_{1,0}F_{1,2} \\ &\quad - 2F_{1,1}^2 + 8F_{0,1}F_{1,0}F_{1,1} + (2F_{0,2} - 6F_{0,1}^2)F_{1,0}^2 \end{aligned} \quad (9)$$

where $F_{i,k} \equiv \langle \frac{N!}{(N-i)!} \frac{N!}{(N-k)!} \rangle$, for i is the number of protons and k is that of anti-protons. The $\hat{\kappa}_n^{(i,k)}$ represents the n -th order correlation function with i protons and k anti-protons. We call it a mixed correlation functions if both i and k are nonzero. Then one can deduce the formulas between cumulants and correlation functions for net-proton:

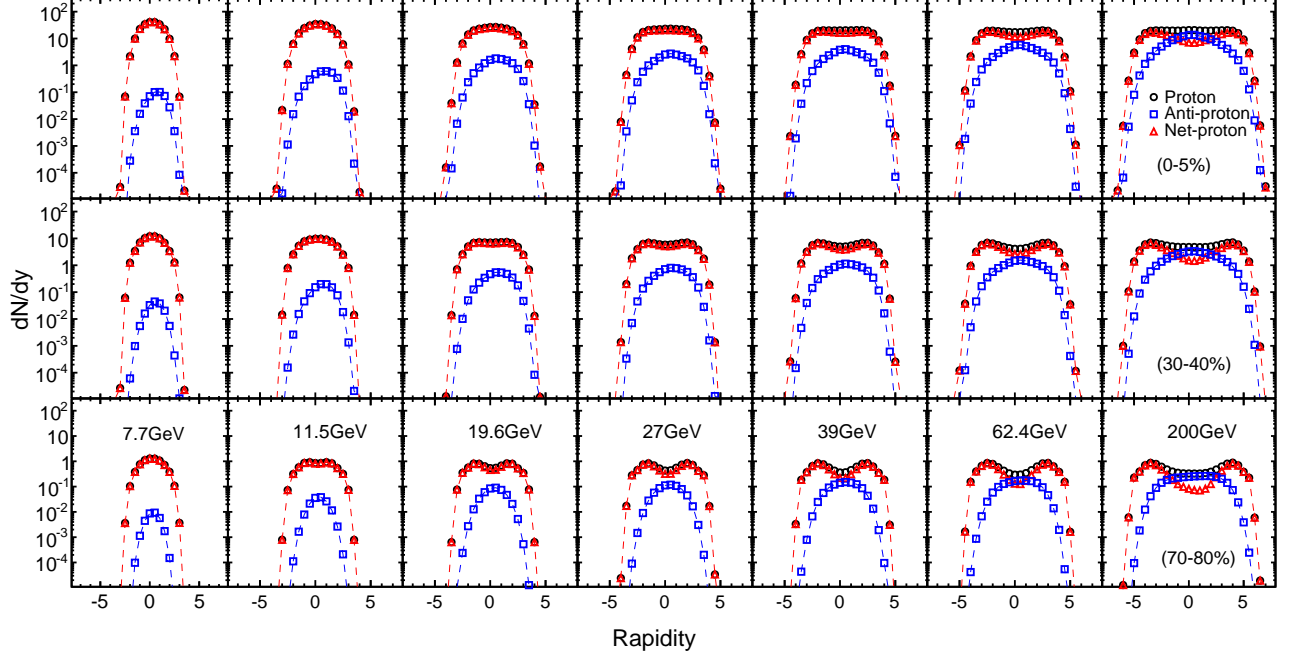


FIG. 1: The rapidity distributions (dN/dy) of proton, anti-proton and net-proton multiplicities in Au+Au collisions at $\sqrt{s_{NN}} = 7.7, 11.5, 19.6, 27, 39, 62.4$ and 200 GeV for three centrality bins (0-5%, 30-40%, 70-80%).

$$C_2 = \langle N \rangle + \langle \bar{N} \rangle + \hat{\kappa}_2^{(2,0)} + \hat{\kappa}_2^{(0,2)} - 2\hat{\kappa}_2^{(1,1)} \quad (10)$$

$$C_3 = \langle N \rangle - \langle \bar{N} \rangle + 3\hat{\kappa}_2^{(2,0)} - 3\hat{\kappa}_2^{(0,2)} + \hat{\kappa}_3^{(3,0)} - \hat{\kappa}_3^{(0,3)} - 3\hat{\kappa}_3^{(2,1)} + 3\hat{\kappa}_3^{(1,2)} \quad (11)$$

$$C_4 = \langle N \rangle + \langle \bar{N} \rangle + 7\hat{\kappa}_2^{(2,0)} + 7\hat{\kappa}_2^{(0,2)} - 2\hat{\kappa}_2^{(1,1)} + 6\hat{\kappa}_3^{(3,0)} + 6\hat{\kappa}_3^{(0,3)} - 6\hat{\kappa}_3^{(2,1)} - 6\hat{\kappa}_3^{(1,2)} + \hat{\kappa}_4^{(4,0)} + \hat{\kappa}_4^{(0,4)} - 4\hat{\kappa}_4^{(3,1)} - 4\hat{\kappa}_4^{(1,3)} + 6\hat{\kappa}_4^{(2,2)} \quad (12)$$

In order to simplify notations used in the discussions on the contributions of different order correlation functions to the fourth-order cumulant in Sec.IV, we make the following definitions according to Eq. (8) for proton and (12) for net-proton, respectively.

$$\begin{aligned} (\hat{\kappa}_2)_p &= 7\hat{\kappa}_2 \\ (\hat{\kappa}_3)_p &= 6\hat{\kappa}_3 \\ (\hat{\kappa}_4)_p &= \hat{\kappa}_4 \\ (\hat{\kappa}_2)_{net} &= 7\hat{\kappa}_2^{(2,0)} + 7\hat{\kappa}_2^{(0,2)} - 2\hat{\kappa}_2^{(1,1)} \\ (\hat{\kappa}_3)_{net} &= 6\hat{\kappa}_3^{(3,0)} + 6\hat{\kappa}_3^{(0,3)} - 6\hat{\kappa}_3^{(2,1)} - 6\hat{\kappa}_3^{(1,2)} \\ (\hat{\kappa}_4)_{net} &= \hat{\kappa}_4^{(4,0)} + \hat{\kappa}_4^{(0,4)} - 4\hat{\kappa}_4^{(3,1)} - 4\hat{\kappa}_4^{(1,3)} + 6\hat{\kappa}_4^{(2,2)} \end{aligned} \quad (13)$$

where $(\hat{\kappa}_n)_p$ represents the n th-order correlation function for proton only and $(\hat{\kappa}_n)_{net}$ is that for net-proton. The scaled numbers in the formulas of $(\hat{\kappa}_n)_p$ and $(\hat{\kappa}_n)_{net}$ are obtained from Eq. (8) for proton and (12) for net-proton.

These numbers reflect the relative contribution of different correlation functions to the fourth-order cumulant.

From the above definitions, we can infer that $(\hat{\kappa}_n)_{net}$ will degrade to be equal to $(\hat{\kappa}_n)_p$ if we omit the contributions of anti-proton. Therefore, in the real data sample, if the measured values of $(\hat{\kappa}_n)_p$ and $(\hat{\kappa}_n)_{net}$ have a clear difference, it means the contribution of anti-proton is important and should be taken into account when calculating correlation functions in that case.

III. AMPT MODEL

A Multi-Phase Transport model with String Melting (AMPT-SM) is a transport model including four main processes: the initial condition, the partonic interactions, the conversion from partonic matter to hadronic matter and the hadronic interactions. The initial condition is obtained from the HIJING model, which includes the spatial and momentum distributions of minijet partons and soft string excitation. Then all the excited strings convert to partons. Scattering among partons are modelled by Zhangs Parton Cascade (ZPC), which at present includes only two-body scattering with cross sections obtained from the pQCD with screening masses. A simple quark coalescence model based on the quark spatial information is used to combine parton into hadrons. The dynamics of the subsequent hadronic matter is described by A Relativistic Transport (ART) model. More details about the AMPT model can be found in Refs [31, 32].

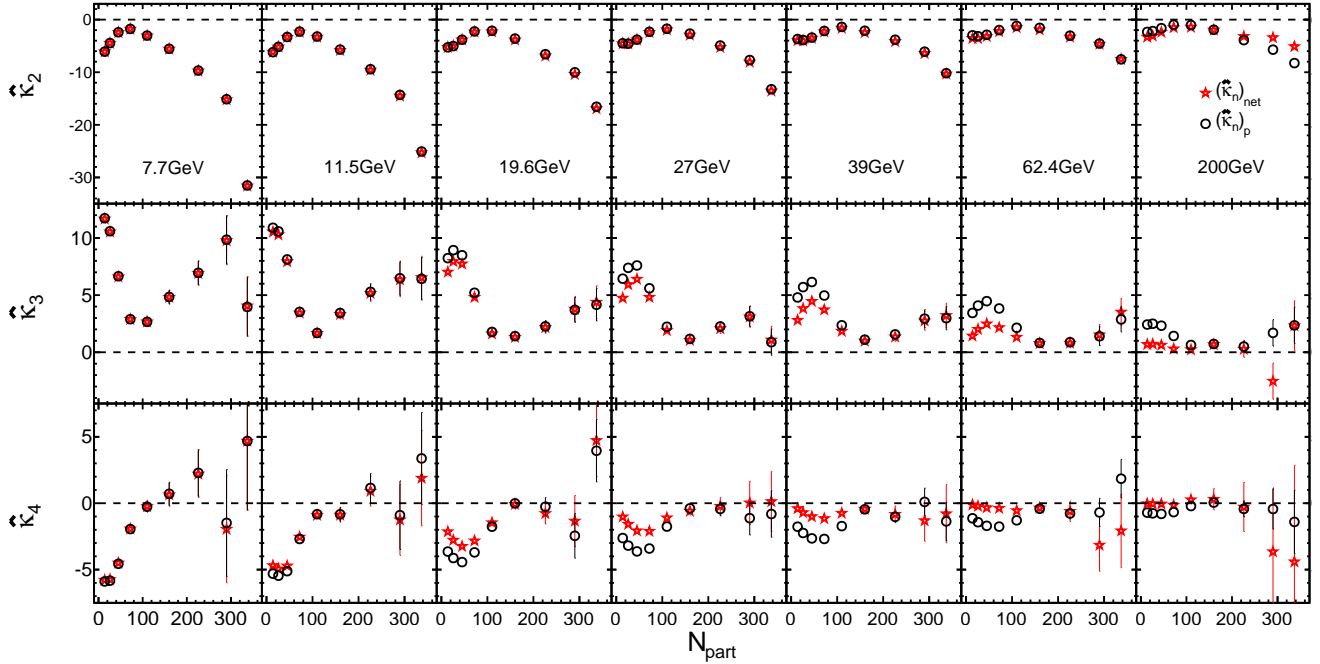


FIG. 2: Centrality dependence of the second-, third- and fourth-order correlation functions of net-proton and proton in Au+Au collisions at $\sqrt{s_{NN}} = 7.7, 11.5, 19.6, 27, 39, 62.4$ and 200 GeV.

In this paper, we perform our calculations with AMPT-SM model in version 2.21 for Au+Au collisions at $\sqrt{s_{NN}}=7.7, 11.5, 19.6, 27, 39, 62.4, 200$ GeV and the corresponding statistics are 23.7, 27.6, 22.5, 21.6, 18.5, 10.5, 8.8 millions, respectively.

IV. RESULTS AND DISCUSSIONS

In the AMPT model calculations, we apply the same kinematic cuts and technical analysis methods as those used in the STAR experiment data [17]. The protons and anti-protons are measured at mid-rapidity ($|y| < 0.5$) and within the transverse momentum range $0.4 < p_T < 2.0$ GeV/c. The centrality is defined by the charged pion and kaon multiplicities within pseudo-rapidity $|\eta| < 1.0$, which can effectively avoid auto-correlation effect in the measurement of cumulants and correlation functions. In order to suppress the volume fluctuations originated from the finite centrality bin width, we apply the centrality bin width correction [33] to the measurement. The statistics error is estimated by Bootstrap method [34, 35].

Figure 1 displays the normalized rapidity distribution (dN/dy) of proton, anti-proton and net-proton in the most central (0-5%), mid-central (30-40%) and peripheral (70-80%) Au+Au collisions at $\sqrt{s_{NN}}=7.7$ to 200 GeV. With the collision energy increases, the dN/dy distributions of proton at central rapidity region monotonically decrease, while those of anti-proton increase with increasing energies. If energy is fixed, the yield of anti-

proton is found to be closer to that of proton in more peripheral collisions. Due to the negligible production of anti-proton at low energies, the dN/dy distribution at central rapidity region of net-proton is observed to be closely follow that of proton. While a clear difference between them can be found at high energies, especially at 200 GeV. These can be explained by the different particle production mechanisms at different RHIC energies. The baryon stopping is more important at low energies, while the pair production dominates the production of proton and anti-proton at high energies.

In Fig.2, we show centrality dependence of various orders of correlation functions for proton and net-proton defined in Eq.(13) at $\sqrt{s_{NN}}=7.7, 11.5, 19.6, 27, 39, 62.4$ and 200GeV. In the first row of the figure, the values of the second-order correlation functions are found to be negative in all centralities and collision energies. The results of net-proton agree well with those of proton when the energies are lower than 200 GeV. At 200 GeV, the values of $(\hat{\kappa}_2)_{net}$ and $(\hat{\kappa}_2)_p$ separate from each other both at peripheral and at central collisions. For the third-order correlations, we see that $(\hat{\kappa}_3)_{net}$ and $(\hat{\kappa}_3)_p$ equal to each other in all centralities only at 7.7 and 11.5 GeV. From 19.6 GeV and above, observable differences between them can be found at peripheral collisions. The differences between net-proton and proton become more obvious with increasing energies. In the third row, we observe that $(\hat{\kappa}_4)_{net}$ are different from $(\hat{\kappa}_4)_p$ from 11.5 GeV and above. From the above behaviors of different order of correlation functions, it infers that the differ-

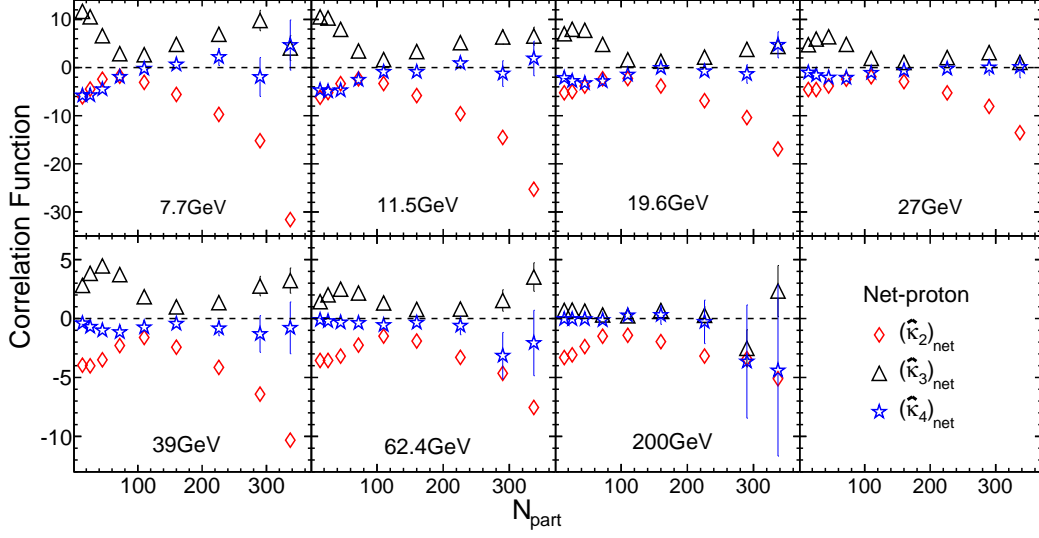


FIG. 3: Centrality dependence of various orders of correlation functions of net-proton in Au+Au collisions at $\sqrt{s_{NN}} = 7.7, 11.5, 19.6, 27, 39, 62.4$ and 200 GeV.

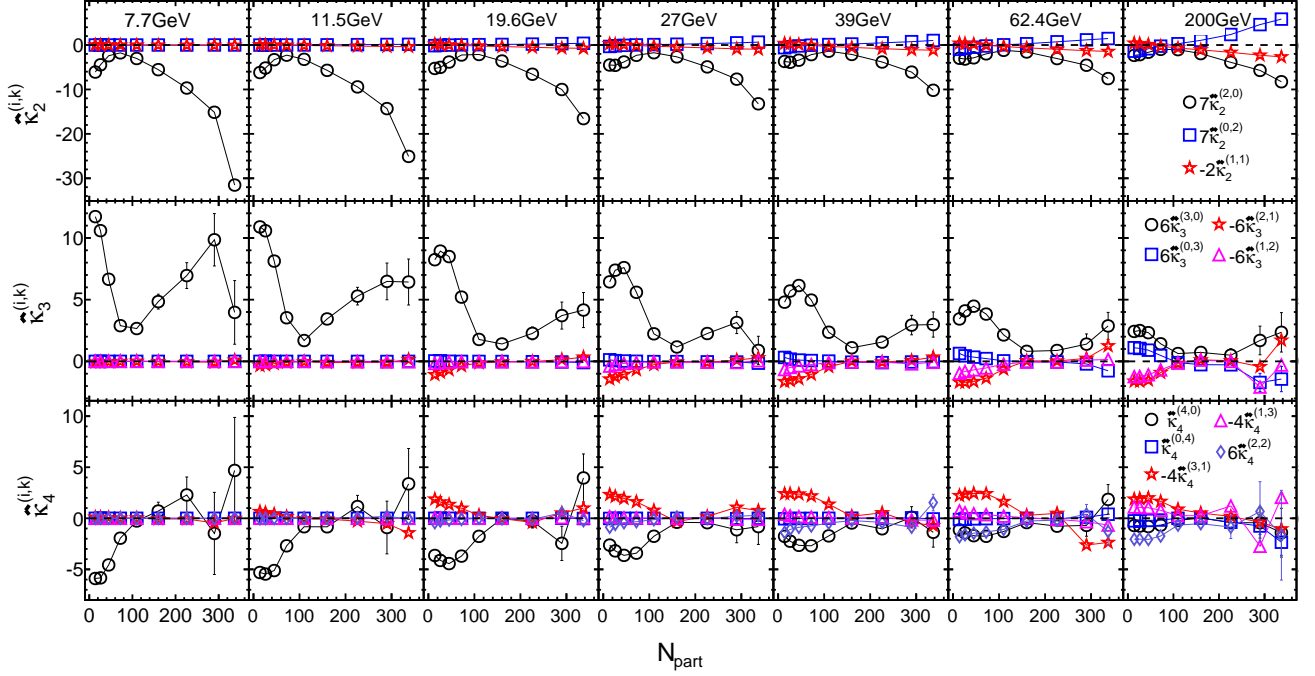


FIG. 4: Centrality dependence of the correlation functions of proton (open circle), anti-proton (open square) and various mixed correlations in Au+Au collisions at $\sqrt{s_{NN}} = 7.7, 11.5, 19.6, 27, 39, 62.4$ and 200 GeV.

ences between net-proton and proton become larger for higher order correlation functions than for lower ones. These differences are caused by the non-negligible contributions from anti-proton.

Figure 3 shows the second-, third- and fourth-order correlation functions of net-proton as a function of cen-

trality at $\sqrt{s_{NN}} = 7.7 - 200$ GeV. Note that this plot can reflect the contributions to the fourth-order cumulant from different orders of correlation functions (12) according to the definitions of Eq. (13). In central collisions, when the energy $\sqrt{s_{NN}} \leq 39$ GeV, we find that the magnitudes of $(\kappa_2)_{net}$ is much larger than those of

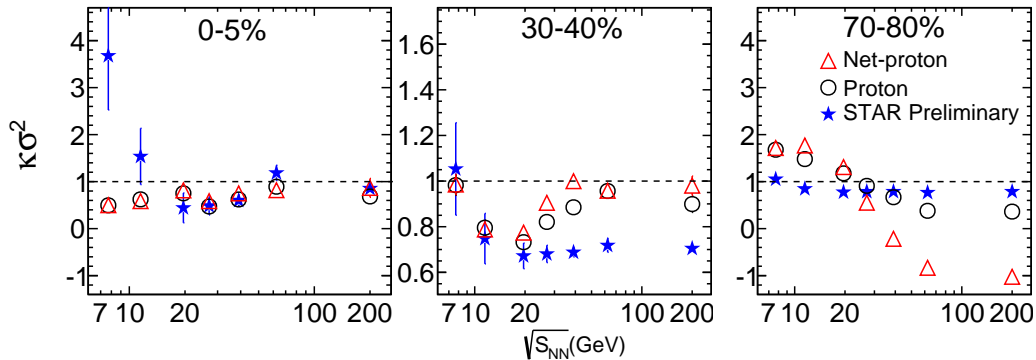


FIG. 5: Energy dependence of cumulant ratio ($\kappa\sigma^2$) of net-proton (open triangle) and proton (open circle) in three centrality bins (0-5%, 30-40%, 70-80%) for Au+Au collisions at $\sqrt{s_{NN}} = 7.7$ to 200 GeV from AMPT model. The solid stars represent the results from STAR experimental data[17].

$(\hat{\kappa}_3)_{net}$ or $(\hat{\kappa}_4)_{net}$. It means that the second-order correlation function is the dominant contribution to the fourth order net-proton cumulant. When the energy increases up to 62.4 or 200 GeV, various orders of correlation functions play comparable roles to the fourth order cumulant. Therefore, higher order correlations should be considered in higher collision energies. On the other hand, in peripheral collisions, there are no obvious dominant orders of correlation functions at all energies.

In figure 4, we compare correlation functions of proton, anti-proton and mixed correlations. Note that we have multiplied correlation functions with the appropriate factors so that they reflect their contribution to the fourth-order cumulant (12). For the second order correlation function, the correlation between protons ($7\hat{\kappa}_2^{(2,0)}$) is clearly the dominant part when the energies $\sqrt{s_{NN}} \leq 39$ GeV. The anti-proton correlation ($7\hat{\kappa}_2^{(0,2)}$) and mix correlation ($-2\hat{\kappa}_2^{(1,1)}$) are around zero and almost flat in all centralities when $\sqrt{s_{NN}} \leq 39$ GeV. But in 200 GeV, the correlation functions of anti-protons or mixed ones have equivalent contribution to those of protons. It implies that anti-proton number must be considered when calculating correlation functions in high RHIC energies. With the orders of the correlation functions increase up to 3rd or 4th, we observe that the roles of anti-protons and mixed correlations get more important both at central and at peripheral collisions. Thus their contributions should not be neglected in the measuring of higher order correlation functions or cumulants in heavy-ion collisions.

In order to make direct comparisons with the STAR measured cumulant ratios [17, 18], in fig. 5 we show the energy dependence of $\kappa\sigma^2$ of proton, net-proton from AMPT model together with those from the STAR experimental results in three centrality bins. For the AMPT calculations, we firstly calculate various correlation functions and then obtain cumulants from Eq.(6)-(8) for proton and (10)-(12) for net-proton, respectively. In the most central collision (0-5%), the results of proton and net-proton from AMPT are almost flat and agree with

each other. In the mid-central collision (30-40%), they start to separate when the energies $\sqrt{s_{NN}} \geq 27$ GeV. In peripheral collision (70-80%), the separation gets larger in high energies. It confirms that the contribution of anti-proton is important in high energies and/or at peripheral collisions in the calculations of cumulants or correlation functions. It can be found that, in the most central collision, the non-monotonic energy dependence of $\kappa\sigma^2$ observed in STAR preliminary results can not be reproduced by the AMPT model. This is because there is no critical physics implemented in the transport model. We also observe that the model can not describe the behaviors of the STAR data either in the mid-central or in the peripheral collisions.

V. SUMMARY

In this paper we have studied various orders of correlation functions of net-proton in Au+Au collisions at $\sqrt{s_{NN}} = 7.7$ to 200 GeV. It is the first time that the contribution of anti-proton is taken into account together with that of proton in calculating correlation functions by using the AMPT model.

We find that the correlation functions from net-proton and proton only have a clear separation at high RHIC energies, especially at peripheral collisions. It infers that the contribution of anti-proton is important in high RHIC energies and/or in peripheral collisions. In central collisions, the magnitude of net-proton correlation functions of the second-order is much larger than those of the higher orders, while they play comparable roles with increasing energies up to 200 GeV. For the centrality dependence of mixed correlations, we observe that proton correlation is the dominant part at low energies. While in high energies, the correlations between anti-protons and the mixed correlations have equivalent contributions to those of protons. It is found that, in the calculation of correlation functions, the contribution from anti-proton

is more important for higher order correlations than for lower ones. The comparison of the cumulants between experimental data and the AMPT calculations shows that the STAR preliminary results can not be described by the AMPT model without implementing critical physics.

The STAR experiment has planned a second phase of the beam energy scan (BES-II) program [36, 37] to run in 2019 - 2020. One of the primary goals of BES-II is the search for evidence of a phase transition between hadronic gas and QGP phases. With significant improved statistics and particle identification in BES-II, it would be of great interests if STAR could measure the correlation functions of net-proton together with high-order cumulant ratios to explore the QCD phase diagram. The results from AMPT model calculations here can provide non-critical estimations for the background contributions

to the QCD critical point search in heavy-ion collisions.

Acknowledgments

We thank Prof. Yuangfang Wu and Xiaofeng Luo for useful discussions and comments. We further thank the STAR collaboration for providing us with their preliminary data. This work is supported in part by the Ministry of Science and Technology (MoST) under grant No. 2016YFE0104800, the Major State Basic Research Development Program of China under Grant No. 2014CB845402, the NSFC of China under Grants No. 11405088, and the Chinese Scholarship Council No. 201506775038.

-
- [1] M. A. Stephanov, K. Rajagopal, and E. V. Shuryak, Phys. Rev. Lett. 81, 4816 (1998).
 - [2] J. Adams *et al.* (STAR Collaboration), Nucl. Phys. A757, 102 (2005).
 - [3] M. Asakawa, U. W. Heinz, and B. Muller, Phys. Rev. Lett. 85, 2072 (2000).
 - [4] V. Koch, A. Majumder, and J. Randrup, Phys. Rev. Lett. 95, 182301 (2005).
 - [5] S. Ejiri, F. Karsch, and K. Redlich, Phys. Lett. B 633, 275 (2006).
 - [6] M. A. Stephanov, Phys. Rev. Lett. 102, 032301 (2009).
 - [7] M. A. Stephanov, Phys. Rev. Lett. 107, 052301 (2011).
 - [8] B. J. Schaefer and M. Wagner, Phys. Rev. D85, 034027 (2012).
 - [9] M. Asakawa, S. Ejiri, and M. Kitazawa, Phys. Rev. Lett. 103, 262301 (2009).
 - [10] M. M. Aggarwal *et al.* (STAR Collaboration), Phys. Rev. Lett. 105, 022302 (2010).
 - [11] L. Adamczyk *et al.* (STAR Collaboration), Phys. Rev. Lett. 112, 032302 (2014).
 - [12] L. Adamczyk *et al.* (STAR Collaboration), Phys. Rev. Lett. 113, 092301 (2014).
 - [13] J. Xu (for the STAR Collaboration), J. Phys. G: Conf. Seri. 736, 012002 (2016).
 - [14] A. Sarkar (for the STAR Collaboration), J. Phys. G: Conf. Seri. 509, 012069 (2014).
 - [15] J. Thader (for the STAR Collaboration), Nucl. Phys. A 956, 320 (2016).
 - [16] A. Adare *et al.* (PHENIX Collaboration), Phys. Rev. C 93, 011901(R) (2016).
 - [17] X. Luo (for the STAR Collaboration), in Proceedings of the 9th International Workshop on Critical Point and Onset of Deconfinement (CPOD 2014): Bielefeld, Germany, Nov. 17C21, 2014, PoS CPOD2014, 019 (2015).
 - [18] X. Luo and N. Xu, Nucl. Sci. Tech. 28, 112 (2017), arXiv:1701.02105.
 - [19] B. Ling and M. A. Stephanov, Phys. Rev. C 93, 034915 (2016).
 - [20] A. Bzdak, V. Koch, and N. Strodthoff, Phys. Rev. C 95, 054906 (2017).
 - [21] A. Bzdak, talks in the Quark Matter 2017: Chicago, USA, Feb. 5-11, 2017.
 - [22] A. Bzdak and V. Koch, arXiv:1707.02640.
 - [23] A. Bzdak and V. Koch, Phys. Rev. C 86, 044904 (2012).
 - [24] R. Esha (for the STAR Collaboration), talks in the Quark Matter 2017: Chicago, USA, Feb. 5-11, 2017.
 - [25] S. He and X. Luo, arXiv:1704.00423.
 - [26] A. Bzdak and P. Bozek, Phys. Rev. C 93, 024903 (2016).
 - [27] A. Bzdak and K. Dusling, Phys. Rev. C 93, 031901(R) (2016).
 - [28] A. Bzdak and K. Dusling, Phys. Rev. C 94, 044918 (2016).
 - [29] L. Adamczyk *et al.* (STAR Collaboration), arXiv:1701.07065.
 - [30] A. Bzdak, V. Koch, and V. Skokov, Eur. Phys. J. C 77, 288 (2017).
 - [31] Z. W. Lin, C. M. Ko, B. A. Li, B. Zhang, and S. Pal, Phys. Rev. C 72, 064901 (2005).
 - [32] Z. W. Lin, arXiv:1403.1854.
 - [33] X. Luo, J. Phys. G: Nucl. Part. Phys. 39, 025008 (2012).
 - [34] B. Efron, R. J. Tibshirani, an introduction to the bootstrap. CRC press, New York, 436, 1994.
 - [35] B. Efron, R. J. Tibshirani, Statistical science, 54 (1986).
 - [36] STAR Collaboration, STAR Note 598, <https://drupal.star.bnl.gov/STAR/starnotes/public/sn0598>.
 - [37] C. Yang (for the STAR Collaboration), talks in the Quark Matter 2017: Chicago, USA, Feb. 5-11, 2017.